bioRxiv preprint doi: https://doi.org/10.1101/2020.04.08.033027; this version posted April 9, 2020. The copyright holder for this preprint (which was not certified by peer review) is the author/funder, who has granted bioRxiv a license to display the preprint in perpetuity. It is made available under aCC-BY-NC-ND 4.0 International license.

Activity dependent translation in astrocytes

Abbreviated Title (40 characters): **Activity dependent translation in astrocytes**

Authors:

D. Sapkota,* [1,2] K. Sakers,* [1,2], Y. Liu[1,2], A.M. Lake[1,2], R. Khazanchi[1,2], R.R. Khankan[3], Y. Zhang[3], & J.D. Dougherty[1,2]

Affiliations:

[1]Department of Psychiatry, Washington University School of Medicine, St. Louis, MO, USA
[2]Department of Genetics, Washington University School of Medicine, St. Louis, MO, USA
[3]Department of Psychiatry and Biobehavioral Sciences, David Geffen School of Medicine, University of California, Los Angeles, CA, USA

*These authors contributed equally

Contact Information:
Dr. Joseph Dougherty
Department of Genetics
Campus Box 8232
4566 Scott Ave.
St. Louis, MO. 63110-1093
P: 314-286-0752
F: 314-362-7855
E:jdougherty@genetics.wustl.edu

Acknowledgements
We thank R. Barve, R. Head and the COMPBIO team for their support. This work was supported by the NIH (5R21DA038458, 1R01NS102272, T32GM008151, and 1K99AG061231). RK was supported by the WUSTL BioSURF program. Key technical resources were supported by NIH through the CTSA (UL1 TR000448) and the Siteman Cancer center (P30 CA91842). Viral vectors were packaged at the Hope Center Viral Vectors Core at Washington University.

Conflict of Interest Statement
JDD has previously received royalties related to the TRAP method.

Word count: Total, including reference and fig legends: 9364, Abstrct: 242, Introduction: 787, Methods: 1875 Results: 2109, Discussion: 1023

Data Availability Statement: Sequencing data are deposited at GEO: GSE147830. Other data are available upon request.

bioRxiv preprint doi: https://doi.org/10.1101/2020.04.08.033027; this version posted April 9, 2020. The copyright holder for this preprint (which was not certified by peer review) is the author/funder, who has granted bioRxiv a license to display the preprint in perpetuity. It is made available under aCC-BY-NC-ND 4.0 International license.

Abstract

Gene expression requires two steps – transcription and translation – which can be regulated independently to allow nuanced, localized, and rapid responses to cellular stimuli. Neurons are known to respond transcriptionally and translationally to bursts of brain activity, and a transcriptional response to this activation has also been recently characterized in astrocytes. However, the extent to which astrocytes respond translationally is unknown. We tested the hypothesis that astrocytes also have a programmed translational response by characterizing the change in transcript ribosome occupancy in astrocytes using Translating Ribosome Affinity Purification subsequent to a robust induction of neuronal activity *in vivo* via acute seizure. We identified a reproducible change in transcripts on astrocyte ribosomes, highlighted by a rapid decrease in housekeeping transcripts, such as ribosomal and mitochondrial components, and a rapid increase in transcripts related to cytoskeleton, motor activity, ion transport, and cell communication. This indicates a dynamic response, some of which might be secondary to activation of Receptor Tyrosine Kinase signaling. Using acute slices, we quantified the extent to which individual cues and sequela of neuronal activity can activate translation acutely in astrocytes. This identified both BDNF and KCl as contributors to translation induction, the latter with both action-potential sensitive and insensitive components. Finally, we show that this translational response requires the presence of neurons, indicating the response is acutely or chronically non-cell autonomous. Regulation of translation in astrocytes by neuronal activity suggests an additional mechanism by which astrocytes may dynamically modulate nervous system functioning.

Keywords

Astrocyte, Translation, TRAP, Regulation, Seizure

Introduction

Transcription of new mRNA and translation of new proteins are both essential for long-term alterations of synaptic strength and efficacy, as well as for the consolidation of memory. This functional role has been extensively shown with classical studies using pharmacological inhibitors in cultures, acute slices and behaving animals (Agranoff et al., 1966; Flexner et al., 1963; Kang and Schuman, 1996). At the transcriptional level, physiological activity, particularly calcium, is known to activate transcription factors such as cyclic AMP response element binding protein (CREB), resulting in a cascade of gene expression changes in neurons and glia (Hardingham et al., 2001; Pardo et al., 2017; Yap and Greenberg, 2018). This involves the initial induction of immediate early genes such as *Fos* and *Jun,* transcription factors which support sustained alterations in synapses by increasing the production of a variety of downstream synaptic transcripts and proteins.

While this transcriptional response has been widely studied, we (Dalal et al., 2017) and others (Chen et al., 2017; Cho et al., 2015) have recently shown that a separate and parallel translational response is also occurring. By sequencing mRNA specifically bound to ribosomes, we assessed the change in occupancy of mRNAs by ribosomes in response to sustained depolarization (Dalal et al., 2017). While increased transcription of a gene often drove a corresponding increase in translation, at least 40% of the variance in translational response was independent of transcript levels. Likewise, Cho et al applied ribosome footprinting to the hippocampi of animals exposed to a fear conditioning paradigm and quantified a substantial translational response (Cho et al., 2015). However, both of these studies were conducted on mixed populations containing a variety of cell types, making the relative contributions of individual cell types difficult to assess. To this end, Chen et al used Translating Ribosome Affinity Purification (TRAP) (Heiman et al., 2008; Sanz et al., 2009) to specifically enrich for ribosomes from hippocampal pyramidal neurons after long term

bioRxiv preprint doi: https://doi.org/10.1101/2020.04.08.033027; this version posted April 9, 2020. The copyright holder for this preprint (which was not certified by peer review) is the author/funder, who has granted bioRxiv a license to display the preprint in perpetuity. It is made available under aCC-BY-NC-ND 4.0 International license.

potentiation, and sequenced the bound mRNA (TRAPseq). The authors identified a time-dependent enrichment of a variety of transcripts on neuronal ribosomes, much of which was undetectable in parallel RNAseq experiments from the same slices(Chen et al., 2017).

Traditionally, most of the transcriptional response to synaptic activity has been presumed to be derived from neurons, as this response can certainly be detected in purified populations of neurons. However, it is well known that other cell types—astrocytes, in particular—also have a response to neuronal activity. Transcriptionally, neuronal maturation directly effects expression of the astrocyte glutamate transporter, *GLT-1* (Perego et al., 2000; Swanson et al., 1997), and other genes (Hasel et al., 2017). Physiologically, astrocytes in the barrel cortex respond with an increase in cytosolic calcium after stimulation of whiskers (Wang et al., 2006). Further, astrocytes increase *Fos* expression in a region-dependent manner (Chai et al., 2017). Chen et al's RNAseq experiment also detected robust changes in transcripts normally associated with glia (Chen et al., 2017). Hasel et al. detected clear induction of astrocyte gene expression when stimulated in co-culture with neurons (Hasel et al., 2017), and single-cell experiments in visual cortex showed astrocytes responding transcriptionally to visual stimulation as robustly as many classes of neurons (Hrvatin et al., 2018).

However, it has not been thoroughly assessed whether or not astrocytes have a programmed *translational* response to cues of neuronal activity. A rapid translational response takes advantage of mRNA already present in the cell to produce new proteins without the time- and energy-consuming process of transcription. Furthermore, as dozens of ribosomes can bind a single transcript, regulation of translation can rapidly amplify protein production. Finally, regulation of translation can also allow for localized production of protein in specific subcellular compartments, a phenomenon that has been profiled in a variety of neurons (Cajigas et al., 2012; Hafner et al., 2019; Ouwenga et al., 2017, 2018; Steward et al., 2015) and now astroglia (Boulay et al., 2017; Pilaz et al., 2016; Sakers et al., 2017).

In this work, we set out to assess whether astrocytes also respond translationally to cues of neuronal activity *in vitro* and *in vivo*. We first use the TRAP method to test the hypothesis that a stimulus known to robustly activate neurons *in vivo*—a pentylenetetrazol (PTZ) induced seizure—will alter translation in astrocytes. We found that hundreds of transcripts alter their ribosomal occupancy within minutes of seizure induction, the vast majority of which had not yet changed transcriptionally. To better understand this result, we next turned to imaging based methods in acute slices to quantify the overall alteration of translation in astrocytes in response to pharmacological manipulations that mimic aspects of neuronal activity. Finally, we replicate these pharmacological studies in primary immunopanned astrocytes and show the bulk of these responses is lost in the absence of neurons.

Materials and Methods

Mouse lines

All procedures were performed in accordance with the guidelines of Washington University's Institutional Animal Care and Use Committee. Mice were maintained in standard housing conditions with food and water provided ad libitum, and crossed at each generation to wildtype C57B6/J mice from Jackson labs. The TRAP line was B6.FVB-Tg(Aldh1L1-EGFP/Rpl10a)^{JD130Htz}, hereafter Astrocyte-TRAP (Doyle et al., 2008).

PTZ treatment and TRAP

Three week old Astrocyte-TRAP mice of both sexes were intraperitoneally injected with PTZ at 60 mg/kg (Sigma P6500, 5 mg/ml stock solution in normal saline). Mice showing persistent convulsions at 8-10 minutes were subjected to rapid decapitation using decapicones (Braintree

bioRxiv preprint doi: https://doi.org/10.1101/2020.04.08.033027; this version posted April 9, 2020. The copyright holder for this preprint (which was not certified by peer review) is the author/funder, who has granted bioRxiv a license to display the preprint in perpetuity. It is made available under aCC-BY-NC-ND 4.0 International license.

Scientific) for harvesting the brains. Control mice were injected with 110 µl normal saline (Sal) and decapitated similarly after 10 minutes. The harvested brains were snap-frozen in liquid nitrogen and stored at −80°C for TRAP. 6 mice, 3 per treatment, were used.

TRAP was performed as descried (Heiman et al., 2008) with a few modifications. Briefly, the brains were homogenized in ice in a buffer (20 mM pH 7.4 HEPES, 150 mM KCl, 5 mM MgCl2, 0.5 mM dithiothreitol, 100 µg/ml CHX, protease inhibitors, and RNase inhibitors). The lysates were cleared by centrifuging at 2000 xg for 10 min at 4°C and treated with DHPC (to 30mM, Avanti) and NP-40 (to 1%, Ipgal-ca630, Sigma) for 5 min in ice. Lysates were further cleared by centrifuging at 20,000 xg for 15 min at 4°C. A 1/10th volume of the cleared lysate was saved as the input control and used to generate RNAseq samples, and the rest was mixed with protein L-coated magnetic beads (Invitrogen), previously conjugated with a mix of two monoclonal anti-GFP antibodies (Doyle et al., 2008), and incubated with rotation for 4 h at 4°C. Beads were washed 5 times with a high-salt buffer (20 mM pH7.4 HEPES, 350 mM KCl, 5 mM MgCl2, 1% NP-40, 0.5 mM dithiothreitol, and 100 µg/ml CHX) and finally resuspended in 200 ul normal-salt buffer (150 mM KCl, otherwise as above).

RNA was extracted from the input and TRAP samples using Trizol LS (Life Technologies) and a purification kit (Zymo Research, R1014) and quality-tested using RNA Pico Chips and BioAnalyzer 2100 (Agilent Technologies). All RINs were >8.

RNAseq and TRAPseq

Libraries were prepared from 1 ug RNA using a library prep kit (NEB #7770), rRNA depletion kit (NEB #E6310), and Ampure XP beads (Beckman #A63881), and following manufacturer's instructions. Prior to sequencing, quality was tested using a High Sensitivity D1000 ScreenTape (Agilent Technologies). Each library was sequenced as 2X150 bp fragments to about 30 million reads of depth using Illumina HiSeq3000 machines.

RNAseq and TRAPseq analysis

Sequencing results were quality-tested using FastQC (version 0.11.7). Illumina sequencing adaptors were removed using Trimmomatic (version 0.38) (Bolger et al., 2014), and reads aligning to the mouse rRNA were removed using bowtie2 (version 2.3.5) (Dobin et al., 2013). Surviving reads were then aligned, using STAR (version 2.7.0d) (Langmead and Salzberg, 2012), to the mouse transcriptome (Ensembl Release 97). The number of reads mapped to each feature were counted using htseq-count (version 0.9.1). All data are available on GEO: GSE147830.

Differential expression analysis was done using edgeR (version 3.24.3) (Robinson et al., 2010). Only genes with > 5 CPM in at least 3 out of 12 samples were retained for further analysis (11,593 genes). A negative binomial generalized log-linear model (GLM) was fit to the counts for each gene. Then the likelihood ratio tests (LRT) were conducted for comparing PTZ samples with Sal samples. The comparisons were listed as follow:

1. $TRAPseq^{PTZ}$ vs $TRAPseq^{Sal}$ = $TRAPseq^{PTZ}$ - $TRAPseq^{Sal}$
2. $RNAseq^{PTZ}$ vs $RNAseq^{Sal}$ = $RNAseq^{PTZ}$ - $RNAseq^{Sal}$
3. $TRAPseq^{PTZ}$ vs $RNAseq^{PTZ}$ = $TRAPseq^{PTZ}$ - $RNAseq^{PTZ}$
4. $TRAPseq^{Sal}$ vs $RNAseq^{Sal}$ = $TRAPseq^{Sal}$ - $RNAseq^{Sal}$
5. $TRAPseq^{All}$ vs $RNAseq^{All}$ = ($TRAPseq^{PTZ}$ + $TRAPseq^{Sal}$) / 2 – ($RNAseq^{PTZ}$ + $RNAseq^{Sal}$) / 2

TRAP-enriched transcripts (Supplemental Table 1) were defined as the union of all transcripts significantly enriched by TRAP (FDR<.1) in the last three comparisons (#3-5). Transcriptionally altered transcripts (Supplemental Table 2), were defined by having FDR<.1 in comparison #2. Translationally altered astrocyte transcripts (Supplemental Table 3) were defined as the intersect

bioRxiv preprint doi: https://doi.org/10.1101/2020.04.08.033027; this version posted April 9, 2020. The copyright holder for this preprint (which was not certified by peer review) is the author/funder, who has granted bioRxiv a license to display the preprint in perpetuity. It is made available under aCC-BY-NC-ND 4.0 International license.

of Supplemental Table 1 with the significant (FDR<.1) transcripts from comparison #1, but removing those that were altered transcriptionally (i.e. also present in comparison #2). Results of all comparisons are included in Supplemental Table 5. Code for these analyses are available on Bitbucket: https://bitbucket.org/jdlabteam/ptz_sal/src/master/RNASeq_analysis/.

qPCR

PTZ and saline treatment, brain harvest, and TRAP were performed as described above. Only mice with a 10-minute seizure response were included. cDNA synthesis, reaction mixture setup, and qPCR were performed as per manufacturer's instructions (QuantaBio #101414, Thermo # A25743, ABI QuantStudio 6Flex). Beta actin was used a loading control. The primers used were as follows:

Beta actin:	Fwd: AGAGGGAAATCGTGCGTGAC, Rev: CAATAGTGATGACCTGGCCGT
Ppp1r9a:	Fwd: AACGTCAGATTCGTTATTGGAC, Rev: CTCTTGTTCCAGGGTCTGG
Sptb:	Fwd: CTTAGAGGATGAGACGCTCTG, Rev: ACAGTTTGCAGATTAGTGCC
Sptan1:	Fwd: CATTGTGAAGCTGGACGAG, Rev: ATTAAACGTGTCCGGATGGT
Sptbn1:	Fwd: TTATTAAGCGCCATGAGGC, Rev: GTAGCTCCAACGTTGTCAG
Islr:	Fwd: CAGTTTGGAGGACGTACCA, Rev: TGGAAGCCATACTTCTCCC
Mapk8ip2:	Fwd: ACCACTGTGAGAAGGACAG, Rev: CCTGGAAATCATCTTGGAAGG
Mbd3:	Fwd: ATGACGACATCAGGAAGCA, Rev: CACATGAGCTAGCATGTCG
CD248:	Fed: ACTTATTTGCCTCCAGTCC, Rev: GATGGGCTTTAGAAGTGGT

Fold changes in response to PTZ were calculated as $2^{-DeltaDeltaCt}$. A mixed linear model (DeltaCt ~ treatment + 1|subject) was constructed, and lme4 package was used in R to test DeltaCt as a function of PTZ treatment. P-value was calculated using likelihood ratio test of the full mixed model with treatment against a model lacking treatment. Three animals per treatment were used.

Gene Ontologies and pathway analysis of translationally regulated genes

We utilized the BiNGO (Maere et al., 2005) tool within Cytoscape to define and plot enrichment of Gene Ontology categories within differentially expressed genes. We utilized the *mus musculus* GOSlim_Generic annotation, inputting either the list of 102 PTZ upregulated or 315 PTZ downregulated (Supplemental Table 3) astrocyte transcripts, and displayed categories reaching 0.05 significance by hypergeometric test after Benjamini-Hochberg correction for multiple testing. We conducted this analysis once in an exploratory setting, using both the whole genome as a reference, and a second time using a more conservative reference of the 3410 astrocyte enriched transcripts (Supplemental Table 1), as highlighted in results. Full GO results are included in Supplemental Data 5. We also examined the same gene lists using the COMPBIO literature mining tool (https://gtac-compbio.wustl.edu/), with default parameters.

Comparison to curated gene lists

TRAP enriched transcripts were compared to prior markers of astrocytes as defined by a pSI < .01 in a prior TRAP experiment (Dougherty et al., 2012), a pSI <.01 of the immunopanned astrocyte expression (Zhang et al., 2014), analyzed as described (Ouwenga et al., 2017), and transcripts with a log2FC of >1, compared to nuclear transcriptomes of both neurons and oligodendrocytes (Reddy et al., 2017). TRAPseq upregulated and downregulated transcripts were further compared to the 102 genes identified by the TADA algorithm (Satterstrom et al., 2018) as causing ASD, and those genes curated as syndromic by the SFARI Gene database (Abrahams et al., 2013), accessed 8/9/19. Finally they were also compared to locally translated transcripts in neurons (Ouwenga et al., 2017) or astrocytes (Sakers et al., 2017). All comparisons were conducted using a Fisher Exact Test, with the maximum number of genes set to the number measurably expressed in the current experiment (11,593).

bioRxiv preprint doi: https://doi.org/10.1101/2020.04.08.033027; this version posted April 9, 2020. The copyright holder for this preprint (which was not certified by peer review) is the author/funder, who has granted bioRxiv a license to display the preprint in perpetuity. It is made available under aCC-BY-NC-ND 4.0 International license.

Imaging based analysis of translation in astrocytes *in vivo*

We sparsely labeled astrocytes, as previously described (Sakers et al., 2017). Briefly, we injected 2µl of AAV9-CBA-IRES-GFP virus (concentration: 10^{12} vector genome (vg) / mL, obtained from the Hope Center Viral Vectors Core at Washington University) in P1-P2 pups bilaterally in the cortex, 1.5mm lateral from the midline in two regions: 1mm caudal to bregma and 2mm rostral to lambda, using a 33g needle (Hamilton #7803-05) with a 50µl Hamilton syringe (#7655-01).

At P21, we prepared acute cortical slices (300µm) in artificial cerebrospinal fluid (aCSF, in mM: 125 NaCl, 25 glucose, 25 $NaHCO_3$, 2.5 KCl, 1.25 NaH_2PO_4, equilibrated with 95% oxygen-5% CO_2 plus 0.5 $CaCl_2$, 3 $MgCl_2$; 320 mOsmol) using a vibratome. 5mM KCl, and 50ng/mL recombinant human/murine/rat BDNF (PeproTech, #450-02) were added to slices with 3µM Puromycin (Tocris #40-895-0) in aCSF and allowed to incubate for 10 minutes at 37°C. In anisomycin condition, 1mM Anisomycin (Sigma #A9789) in aCSF was added to slices 30 minutes before Puromycin at 37°C. We fixed slices with 4% paraformaldehyde in PBS for 30 minutes, followed by 30 minutes in 30% sucrose and freezing in OCT (Sakura #4583) for cryosectioning.

We cryosectioned 40µm sections into PBS and incubated with Chicken Anti-GFP (Aves, 1:1000), and Mouse Anti-PMY (Kerafast, 1:1000) at room temperature, followed by detection with appropriate Alexa conjugated secondary antibodies (Invitrogen), and counterstained nuclei with DAPI. We performed confocal microscopy on an AxioImager Z2 (Zeiss). Representative images are from 2-3 animals per condition with cell N indicated in the figure legends.

Fluorescence intensity of PMY and GFP area were quantified using custom macros in ImageJ (NIH) and subsequently analyzed in R 3.4.1 software. Data were analyzed by Anova using the car package in R and post-hoc pairwise t-tests with Bonferroni correction for multiple comparisons.

Imaging based analysis of translation in astrocytes *in vitro*

We purified postnatal rat astrocytes according to previously published immunopanning protocol (Foo et al., 2011; Li et al., 2019; Zhang et al., 2016). First, we coated separate immunopanning dishes (150 mm) with antibody against CD45 (BD 550539), Itgb5 (eBioscience 14-0497-82), and a hybridoma supernatant against the O4 antigen (Zhang et al., 2016). Next, we dissected cerebral cortices from postnatal day 3 rat pups and digested the tissue into a single cell suspension using papain. We incubated dissociated cells sequentially on the CD45 and O4-coated panning dishes to remove microglia/macrophages and oligodendrocyte precursor cells. We isolated astrocytes by incubating the single cell suspension on the Itgb5-coated panning dish. After washing away non-adherent cells, we lifted astrocytes bound to the Itgb5-coated dish using trypsin and plated them on poly-D-lysine coated plastic coverslips in a serum free medium containing Dulbecco's modified Eagle's medium (DMEM) (LifeTechnologies 11960069), Neurobasal (LifeTechnologies 21103049), sodium pyruvate (LifeTechnologies 11360070), SATO (Foo et al., 2011), glutamine (LifeTechnologies 25030081), N-acetyl cysteine (Sigma A8199) and HBEGF (Sigma E4643) on 24-well culture plates. We replaced half of the medium with fresh medium every 2-3 days.

We added AAV9-GFAP-LCK-CFP-MYC virus (concentration: 10^{11} vg / mL) to each well of rat astrocytes after 2 days *in vitro*. We changed the medium 24 hours after infection and analyzed cells 5 days after infection to obtain ~30% sparse labeling prior to puromycylation. Astrocytes were treated with drugs in the same manner as acute slices with the following additions: KCl was tested at both 5mM and 50mM, Tetrodotoxin (TTX) was tested at 1µM (Abcam #120055) with and without KCl, and untreated wells were used as control. Duration of treatment was identical to

bioRxiv preprint doi: https://doi.org/10.1101/2020.04.08.033027; this version posted April 9, 2020. The copyright holder for this preprint (which was not certified by peer review) is the author/funder, who has granted bioRxiv a license to display the preprint in perpetuity. It is made available under aCC-BY-NC-ND 4.0 International license.

acute slices methods, followed by two washes with fresh media and immediate 4% paraformaldehyde fixation.

We permeabilized coverslips with 0.2% Triton X100 and blocked with 10% donkey serum concurrently. Then incubated coverslips with blocking solution, rabbit anti-GFAP (Dako, 1:1500), and mouse anti-PMY (Kerafast, 1:1000) overnight at 4°C, followed by detection with appropriate Alexa conjugated secondary antibodies (Invitrogen, 1:1000), and counterstained nuclei with DAPI. We acquired 5-10 images per well on a Zeiss Imager.M2 microscope with an AxioCam M Rm camera. Three independent experiments were conducted. Fluorescence intensity of PMY signal was quantified by drawing ROIs around individual cells using ImageJ (NIH) and analyzed using R as above.

Results

Acute seizure activity alters ribosome occupancy of transcripts in astrocytes *in vivo*

A fundamental aspect of astrocyte function in the CNS is sensing and responding to neuronal activity (Charles et al., 1991; Perea et al., 2009; Schipke and Kettenmann, 2004). Indeed astrocytes respond transcriptionally, morphologically and functionally to the presence of neurons and neuronal activity (Hasel et al., 2017; Hrvatin et al., 2018) but whether changes in their translatome also occur remains mostly unexplored. Therefore, we set out to determine if a robust induction of neural activity would acutely alter the profile of mRNAs bound to ribosomes in astrocytes *in vivo*.

We induced seizure in Astrocyte-TRAP mice, which express GFP-tagged ribosomes in all astrocytes **(Fig. 1a,** and (Doyle et al., 2008)), using PTZ, and harvested brains after 8 - 10 minutes from the seizing mice and saline injected controls **(Fig. 1b)**. We focused on a single, short time interval with the intention to isolate the translational response independent of subsequent transcription. We collected both transcripts bound to astrocyte ribosomes via the TRAP method, as well as a parallel total RNAseq from each sample, and sequenced all samples to a depth of 28-43 million reads. Multidimensional scaling analysis shows that samples cluster on one axis strongly by whether they are from TRAP or RNAseq, and another axis by whether the TRAP samples come from PTZ or Saline treated mice, confirming reproducibility of the method and indicating a robust translational response is occurring on astrocyte ribosomes **(Fig. 2a)**. We next compared the TRAPseq samples to the RNAseq and confirmed TRAP to define astrocyte translated transcripts **(Fig. 2b, Suppl Table 1)**, and this profile was significantly enriched for transcripts enriched by prior TRAP studies (Dougherty et al., 2012), immunopanning (Zhang et al., 2014), and nuclear sorting based assessments of *in vivo* astrocyte gene expression (Reddy et al., 2017) (all p<10E-16 by Fisher's Exact Test). Thus, we are confident we have measured ribosome-bound mRNAs from astrocytes in stimulated and unstimulated animals.

Next, we leveraged this data to determine whether transcripts alter their ribosome occupancy in response to this stimulation. First, we tested our assumption that using a short interval would allow us to exclude most of the transcriptional response by directly comparing the PTZ and Saline RNAseq data. In fact, there were a few genes that did show a significant transcriptional response, even within 8-10 minutes **(Fig. 2c, Suppl Table 2)**; however, these were only a very small number (23, at FDR<.1), and unsurprisingly these were largely immediate early genes (e.g. *Npas4*, Log2FC= 2.2, FDR<2E-11, *Fos* Log2FC=1.8, FD<1.3E-18, *Arc*, Log2FC=1.02, FDR<1.6E-6) known to transcriptionally respond to neuronal activity. We next contrasted this with the number of transcripts with altered ribosome occupancy by comparing PTZ-TRAP to Saline-TRAP **(Fig. 2d)**. Because TRAP is an enrichment, but not perfect purification of astrocyte RNA, we conservatively filtered these to only pursue those transcripts that were also enriched by TRAPseq over RNAseq, as well as removed those that showed a transcriptional

bioRxiv preprint doi: https://doi.org/10.1101/2020.04.08.033027; this version posted April 9, 2020. The copyright holder for this preprint (which was not certified by peer review) is the author/funder, who has granted bioRxiv a license to display the preprint in perpetuity. It is made available under aCC-BY-NC-ND 4.0 International license.

response, resulting in 417 transcripts **(**FDR<.1,**Suppl Table 3,** also see **Fig 2e** and **Suppl. Table 4** for all transcripts and comparisons). Most of these showed only minimal changes in translation as we limited PTZ action to 8-10 minutes in order to focus exclusively on acute response— for instance, only four transcripts exhibited a fold change ~1.5. Yet, using qPCR, we could independently confirm these nominal changes for a majority of the candidates tested **(Fig. 2f).** We confirmed 5 out of 5 upregulated (*Mapk8ip2*, *Sptan1*, *Sptbn1*, *Sptb*, and *Ppp1r9a*) and 1 out of 3 downregulated (*CD248*, but not *Islr* and *Mdb3* although the latter two still showed the expected trend) candidates, and clearly found PTZ treatment as the factor driving these translational changes (p>0.05). Thus, overall we discovered that astrocytes do have a robust translational response to stimulation *in vivo*, with at least 417 of 3410 the astrocyte-enriched transcripts altering their ribosome occupancy, and with a larger proportion decreased (n=315) rather than increased (n=102) occupancy (Fig. 2e). Thus, a stimulation induces immediate changes in astrocyte ribosome occupancy.

We then applied pathway analyses to these data to better infer potential functions for the astrocytic translational response after seizure. First, examining the downregulated genes, the gestalt view provided by this analysis suggests a decrease in ribosomal occupancy of a variety of metabolic pathways **(Fig. 3a)**. For example, ribosomal transcripts are immediately downregulated (p<3.03E-07, hypergeometric test, B-H corrected), as are key transcripts utilized by mitochondria (p<8.37E-14), including numerous members of the electron transport chain. This suggests that robust activity in neurons triggers an immediate shift of protein production in astrocytes for housekeeping and metabolic functions. Next, we examined the upregulated genes and found robust increases in ribosome occupancy for transcripts involved in the cytoskeleton (p< 1.16E-10), notably actin binding proteins (p<1.27E-08), as well as a variety of motor proteins (p<9.68E-06), and ion transporting proteins (p<1.19E-05) **(Fig. 3b) (Suppl Table 5)**. The translational upregulation of cytoskeleton family transcripts suggests that an increase in neuronal activity poises the astrocyte for increased perisynaptic process motility. This supports a previous finding demonstrating that an increase in calcium induces astrocyte process motility (Molotkov et al., 2013). Further, the overrepresentation of transcripts in ion transport suggest a homeostatic response to excessive neurotransmitter release induced by the seizure. Taken together, this pathway analysis points toward a mechanism for astrocytes to control excessive ions and neurotransmitter in the extracellular space.

Transcript specific regulation of translation is often mediated by the interaction of RNA-binding proteins with specific sequences or RNA secondary structures, most often found in the 5' and 3' untranslated regions (UTRs). We therefore tested the hypothesis that the regulated genes shared particular sequence motifs. First we examined the broad features of the 5' and 3' UTRs and found that the upregulated transcripts generally had UTRs with a longer length and a higher GC content (implying more stable secondary structures) than the downregulated transcripts **(Fig. S1a-d)**. Emboldened to consider the UTRs as being responsible for some of the transcript specific regulation, we then tested the hypothesis that there are specific motifs shared across transcripts. We utilized the AME tool within MEME suite (McLeay and Bailey, 2010) to screen for known vertebrate RNA-binding protein (RBP) target motifs in the upregulated and downregulated transcripts, and then compared their abundance. At FDR <.1, we found dozens of potential regulatory motifs differing between the sets, which could be grouped into families based on their sequence similarity **(Fig. S1e,f).** This suggests that the regulation of translation of these transcripts is mediated by sequences found in the UTR elements.

Finally, we sought to identify signaling pathways that might be upstream of these translationally regulated genes. We leveraged the COMPBIO tool for contextual language processing to mine Pubmed with the lists of translationally regulated genes and identify and

bioRxiv preprint doi: https://doi.org/10.1101/2020.04.08.033027; this version posted April 9, 2020. The copyright holder for this preprint (which was not certified by peer review) is the author/funder, who has granted bioRxiv a license to display the preprint in perpetuity. It is made available under aCC-BY-NC-ND 4.0 International license.

cluster themes related to their gene products (https://gtac-compbio.wustl.edu/). COMPBIO reproduced aspects of the GO analysis, including themes related to ribosomes, cytoskeleton, and mitochondria. Beyond what was found by GO, it highlighted a surprising connection to neurodegenerative diseases driven by the Huntington-related genes *Htt* and *Smcr8* as well as some forms of intellectual disability driven by the neurofibromatosis genes *Nf1* and *Nf2*, and the Cornelia de Lange syndrome genes *Smc3* and *Nipbl*. Indeed, the upregulated transcripts were significantly enriched in both recently empirically identified *de novo* autism genes (Fisher's Exact Test, $p< 0.0003$) (Satterstrom et al., 2018), and a curated list of syndromic ASD/ID genes ($p< 0.05$) (Abrahams et al., 2013). Finally, this analysis also highlighted Ras and MAPK kinase signaling **(Fig. S2)**. These well studied intracellular signaling pathways are known to be downstream of neuronal activity-induced neurotrophic factors, such as BDNF. BDNF is a known regulator of translation and synaptic plasticity in neurons (Leal et al., 2014), and astrocytes are also known to express BDNF receptors and respond to BDNF (Aroeira et al., 2015; Colombo et al., 2012; Wang et al., 1998). For example, astrocytes have previously been reported to increase nitric oxide production in response to BDNF (Colombo et al., 2012), and indeed, we see increased ribosome occupancy of the key synthetase gene (*Nos1*) following stimulation, and others have detected an increase in global translation in astrocytes following BDNF stimulation in co-culture with neurons (Müller et al., 2015). We therefore turned to an imaging-based analysis of translation to assay this and other molecular signals that might directly induce a translational response in astrocytes.

Astrocytes respond translationally to cues of neuronal activity in acute slices

While our TRAP experiment demonstrates that a seizure-inducing stimulus can alter ribosome occupancy of transcripts, we cannot directly image new translation this way. Furthermore, stimulated neurons produce a variety of cues that could induce translation, and it is unclear which one(s) of these the astrocytes may be responding to. Therefore, we set out to assess how neuronal activity alters astrocyte translation acutely by exposing acute brain slices to pharmacological manipulations that trigger or mimic aspects of neuronal activity, and measuring global translation in sparsely labeled astrocytes **(Fig. 4a)**. We first investigated whether BDNF also stimulated translation of astrocyte transcripts in acute slices via immunofluorescent quantification of short-pulse puromycin (PMY) incorporation into sparsely labeled astrocytes. Puromycin incorporates into the extending peptide chain on the translating ribosome and thus tags ongoing translation with an epitope that can be immunofluorescently detected. BDNF induced a robust increase in puromycylation in astrocytes **(Fig. 4b,c)**. This is consistent with increased translation, as preincubation with another inhibitor of translation, anisomycin, blocked any PMY signal. BDNF transcription and secretion is regulated by neuronal activity (Balkowiec and Katz, 2000; Dieni et al., 2012; Zafra et al., 1990) and thus we hypothesized that globally altering neuronal firing regulates astrocyte translation. Therefore, we next depolarized the slices using 5 mM KCl, a manipulation known to depolarize neurons and increase action potential frequency. KCl alone also robustly increased puromycin incorporation in astrocytes, indicating that increased neuronal firing stimulates nascent protein synthesis in astrocytes **(Fig. 4b)**. Consistent with previous reports (Song and Gunnarson, 2012), we noted an increase in cell size after treatment with KCl **(Fig. S3**) suggesting that water permeability is also increased in astrocytes during KCl treatment, leading to cell swelling. However, even after normalizing the PMY intensity to cell size, quantified by astrocyte-GFP area, we still detected a robust increase in translation **(Fig. 4c)**. This argues against the possibility that increased cell size explains the greater PMY intensity. We next asked the reciprocal question of whether silencing neuronal firing results in a concomitant decrease in astrocyte translation by blocking all neuronal activity using tetrodotoxin (TTX). TTX alone significantly decreased puromycylation in astrocytes, suggesting at least some of the basal level of translation in astrocytes is dependent on spontaneous activity

bioRxiv preprint doi: https://doi.org/10.1101/2020.04.08.033027; this version posted April 9, 2020. The copyright holder for this preprint (which was not certified by peer review) is the author/funder, who has granted bioRxiv a license to display the preprint in perpetuity. It is made available under aCC-BY-NC-ND 4.0 International license.

of surrounding neurons. However, activity-independent translation also occurs in astrocytes because TTX-treated slices still contained significantly more puromycylation compared to anisomycin-treated slices. Because KCl will also depolarize astrocyte membranes, we next investigated whether the induction of astrocyte translation by KCl was dependent on neuronal firing and subsequent neurotransmitter release. Therefore, we blocked neuronal firing with TTX prior to KCl stimulation. Indeed, pairing KCl treatment with TTX significantly inhibited most of the KCl induced increase in translation. However, translation was still higher than when TTX was used alone. Thus, these findings suggest that KCl-induced translation in astrocytes has components that are both dependent and independent of neuronal activity.

Activity-dependent astrocyte translation is non-cell autonomous

The TTX experiments above provided some evidence that the presence of neurons and neuronal activity was largely required for the KCl response in astrocyte translation. We further tested this hypothesis by separating astrocytes from neurons and assessing their translational response to the same panel of chemical modulators **(Fig. 5a)**. We utilized a primary culture system in which mature astrocytes are immunopanned from dissociated rat cortices (Foo et al., 2011; Zhang et al., 2016). In this system, astrocytes exhibit morphological, physiological, and transcriptional profiles similar to those *in vivo* and thus make for a more direct comparison to our *ex vivo* data than traditionally cultured astrocytes. As before, we found that 1mM anisomycin was sufficient to block puromycin signal in this system **(Fig. 5b,c)**. However, we found no other manipulation resulted in a significant upregulation on puromycin signal *in vitro*. Indeed, in contrast to our original findings, we found a modest but significant down regulation of translation when astrocytes were treated with BDNF. This finding is supported by previous work using comparable methods, supporting the idea that astrocyte translational regulation is mediated by neuronal firing and/or neuronal contact (Müller et al., 2015). Further, we found another modest yet significant decrease in translation from the combination of KCl and TTX, but no effect of either TTX or KCl alone **(Fig. 5b,c)**. Together, these data suggest that activity-dependent signaling from neurons controls astrocyte translation.

Discussion

Proper nervous system development and function requires precise spatiotemporal translation of proteins. Recently, there has been a focus on identifying transcriptional programs correlated with important developmental milestones (Kalish et al., 2018) and neuronal activity (Hrvatin et al., 2018). Neuronal activity can also induce such transcription in a cell-autonomous fashion which has been shown to be important for synaptic plasticity and is classically mediated through activation of factors such as CREB (Yap and Greenberg, 2018). While CREB also induces activity-dependent transcriptional changes in astrocytes (Hasel et al., 2017; Pardo et al., 2017), neuronal activity-regulated translation in astrocytes has been mostly overlooked. Here, we show in acute slices that overall astrocyte translation changes after treatment with neuronal activity modulators but occurs only in the presence of neurons. In agreement with our findings, a study using FUNCAT (Dieterich et al., 2010), an analogous method to puromycylation, found similar results of BDNF *in vitro* on astrocyte translation (Müller et al., 2015). Further, we profiled the changes in ribosome occupancy in astrocytes acutely after induction of seizure by TRAPseq and found a robust translational response, with hundreds of transcripts showing regulation. Pathway analyses highlight independent roles for upregulated and downregulated genes, and analyses of sequence features indicate that some of this regulation may be driven by shared motifs in UTR sequences. Finally, several genes involved in ASD, including several that are known to be quite dose sensitive, appear to show acute regulation of translation in astrocytes in response to neuronal activity.

bioRxiv preprint doi: https://doi.org/10.1101/2020.04.08.033027; this version posted April 9, 2020. The copyright holder for this preprint (which was not certified by peer review) is the author/funder, who has granted bioRxiv a license to display the preprint in perpetuity. It is made available under aCC-BY-NC-ND 4.0 International license.

The current study does have some limitations that should be mentioned. First, TRAP is a method for enrichment, but not perfect purification. Therefore, we conservatively limited our analysis for translationally regulated transcripts to those that were significantly enriched in astrocytes. It is possible that with additional strategies for enrichment, we might be able to identify even more transcripts that are changing ribosome occupancy. However, even with the current criteria we were still able to identify hundreds of transcripts. It is also worth mentioning that while assessment of ribosome occupancy does indicate regulation of translation, it is not necessarily identical to measurement of actual nascent protein production. Indeed, increased signal in TRAP might reflect an increase in stalled ribosomes on a given transcript rather than a recruitment of new ribosomes and increased translation. Thus, one should be cautious about inferring direction of changes in protein levels from changes in TRAP alone.

Nonetheless, it is clear from this study that astrocytes have a robust and transcript-specific translational response to neuronal activity. It is interesting to note that both BDNF and KCl can induce translation in astrocytes, and that the KCl induction has components that are both dependent and independent of neuronal firing, as shown by TTX block. This may mean that there are discrete transcripts regulated by each neuronal signal, perhaps secondary to distinct secondary messenger events. This is supported by the discovery of motifs in subsets of the transcripts. We found motifs for over a dozen different RBPs in each transcript list – more than could be readily pursued experimentally here. Further, as many of these motifs are quite similar across RBPs, it can be a challenge to identify which, if any, of the known RBPs might be playing a role in this particular context. Nonetheless, it is possible that a RBP molecular code is defined by discrete signaling pathways which upon activation ultimately alter translation of specific transcripts downstream of each RBP. On the other hand, there could be a more non-specific mechanism where a variety of RBPs have redundant roles and work in a larger ensemble. For example, the set of RBPs identified as enriched in the upregulated transcripts is remarkably similar to the motifs found in our recent study of Celf6 binding targets (Rieger et al., 2018), even though the actual transcripts are distinct. As Celf6 and related Celf proteins have a role in forming RNA granules for mRNA storage and/or decay, and these granules often contain numerous species of RBPs and mRNAs interacting non-specifically through phase separation mediated by disordered domains, this suggests that transcripts enriched in binding for this selection of proteins may be more likely sequestered into a common granule awaiting some kind of signal for release and translation following neuronal activation. What is common to both studies is that there was a GC bias in both lists, and thus there could be some shared preference for GC binding RBPs in both cases. More sophisticated microscopy to track individual mRNAs, and perhaps a targeted proteomics study of some of these proteins in the context of astrocytes, might be able to elucidate which RBPs play a role in the regulation described here. This could eventually help test whether distinct signals regulate distinct transcripts or rather there is a more coordinated action across RBPs.

Finally, it is also interesting to consider the relationship between global translation regulation and the potential for local translation regulation at peripheral processes and endfeet (Boulay et al., 2017; Sakers et al., 2017). Because it was previously uncharacterized, we focused here only on global analyses of translation in the whole astrocyte. However, it is intriguing that there is a highly significant overlap ($p<10E-16$, Fisher's Exact Test) between the transcripts identified here, particularly those that are downregulated, and those previously described as bound to astrocyte ribosomes in perisynaptic fractions (Sakers et al., 2017). This suggests that some of these transcripts may be stalled on ribosomes in the periphery awaiting some signal secondary to neuronal activation, at which point they are rapidly translated and the RNA is subsequently degraded, similar to what has been reported for Arc in neurons (Farris et al., 2014). This could provide a substrate for local and activity dependent production of certain proteins in

bioRxiv preprint doi: https://doi.org/10.1101/2020.04.08.033027; this version posted April 9, 2020. The copyright holder for this preprint (which was not certified by peer review) is the author/funder, who has granted bioRxiv a license to display the preprint in perpetuity. It is made available under aCC-BY-NC-ND 4.0 International license.

specific processes of a given astrocyte. This would of course require a highly localized signal to activate such translational activity in a process-specific manner. Candidates could be calcium transients in microdomains, or regions of elevated kinase activity downstream of G-protein Coupled Receptors or Receptor Tyrosine Kinase cell surface receptors such as those activated by BDNF. Our findings here motivate future studies aimed at understanding the potential for subcellular localization of activity dependent translation in astrocytes.

bioRxiv preprint doi: https://doi.org/10.1101/2020.04.08.033027; this version posted April 9, 2020. The copyright holder for this preprint (which was not certified by peer review) is the author/funder, who has granted bioRxiv a license to display the preprint in perpetuity. It is made available under aCC-BY-NC-ND 4.0 International license.

Figures

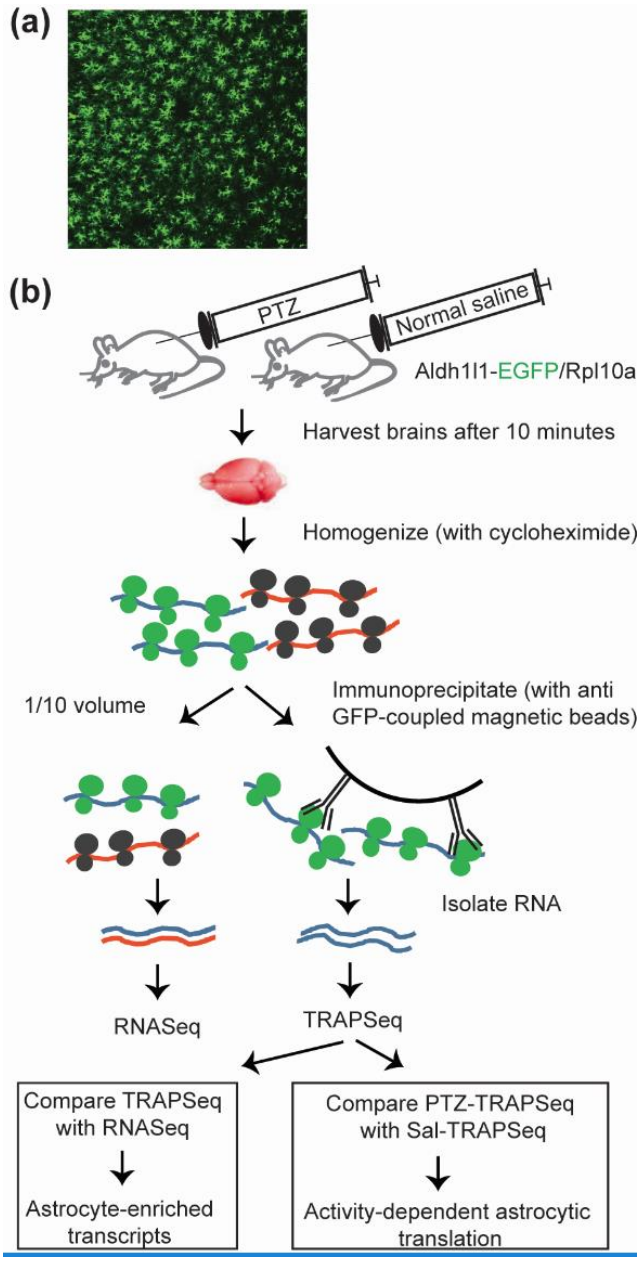

Figure 1: Illustration of experimental design

a) Representative image of an Astrocyte-TRAP mouse showing extensive expression of the GFP-tagged ribosome construct in astrocytes across the cortex.

b) Illustration of the experimental paradigm for harvesting mRNA bound to astrocyte ribosomes, with and with seizure induction.

bioRxiv preprint doi: https://doi.org/10.1101/2020.04.08.033027; this version posted April 9, 2020. The copyright holder for this preprint (which was not certified by peer review) is the author/funder, who has granted bioRxiv a license to display the preprint in perpetuity. It is made available under aCC-BY-NC-ND 4.0 International license.

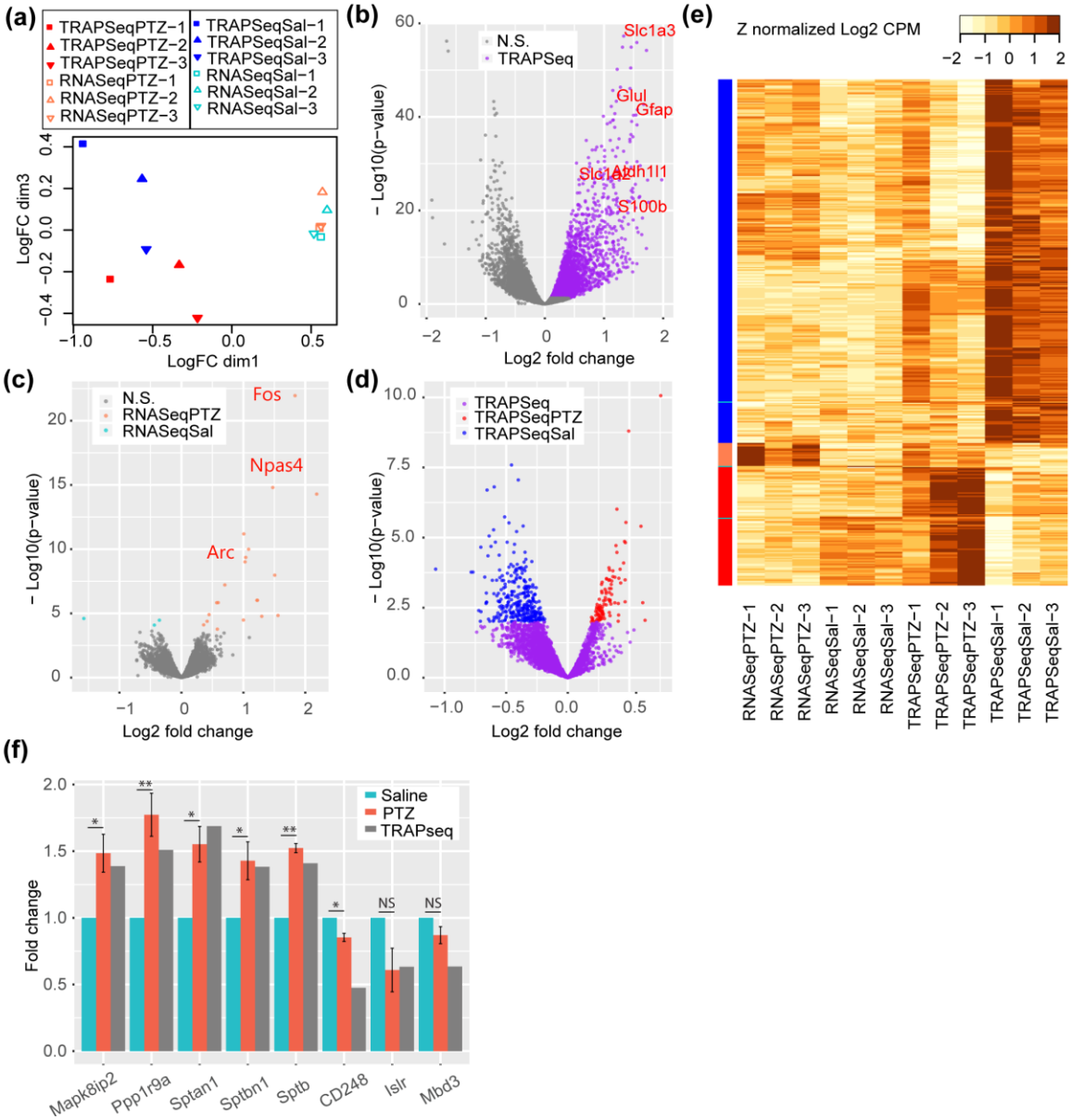

Figure 2: Seizure rapidly alters the translational profile of astrocytes.

a) Multidimensional scaling of twelve samples shows astrocyte TRAPseq samples are clearly separated from RNAseq samples, and that stimulated and unstimulated TRAPseq samples are also distinguished in this unsupervised clustering approach.

b) Volcano plot of comparison of all TRAP samples to all RNAseq samples defines transcripts enriched on astrocyte ribosomes (purple) and these include known markers of astrocytes (red genes) as expected.

c) Volcano plot comparing RNAseq from stimulated and unstimulated animals identifies the subset of transcripts responding rapidly to seizure induction (orange and blue transcripts, FDR<.1). Some of the immediate early genes are marked.

bioRxiv preprint doi: https://doi.org/10.1101/2020.04.08.033027; this version posted April 9, 2020. The copyright holder for this preprint (which was not certified by peer review) is the author/funder, who has granted bioRxiv a license to display the preprint in perpetuity. It is made available under aCC-BY-NC-ND 4.0 International license.

d) Volcano plot comparing TRAPseq from stimulated and unstimulated animals identifies the subset of the TRAP enriched transcripts (purple) that were upregulated (red) or downregulated (blue) by seizure (FDR<.1).

e) A heatmap of Z-normalized data for all transcriptionally upregulated (demarked by orange bar on left) or downregulated (cyan bars) transcripts, and astrocyte translationally downregulated (blue bar) or upregulated (red bar) transcripts across all conditions.

f) qPCR validates translational changes in independent samples. PTZ- and saline-treated mice were subjected to TRAP followed by qPCR, and fold changes calculated as $2^{-DeltaDeltaCt}$. Mixed linear model followed by likelihood ratio test was used to test DeltaCt as a function of PTZ treatment. Corresponding TRAPseq results are included for comparison. N=3 mice per treatment. *, p-value ≤0.05; **, p-value ≤0.01

bioRxiv preprint doi: https://doi.org/10.1101/2020.04.08.033027; this version posted April 9, 2020. The copyright holder for this preprint (which was not certified by peer review) is the author/funder, who has granted bioRxiv a license to display the preprint in perpetuity. It is made available under aCC-BY-NC-ND 4.0 International license.

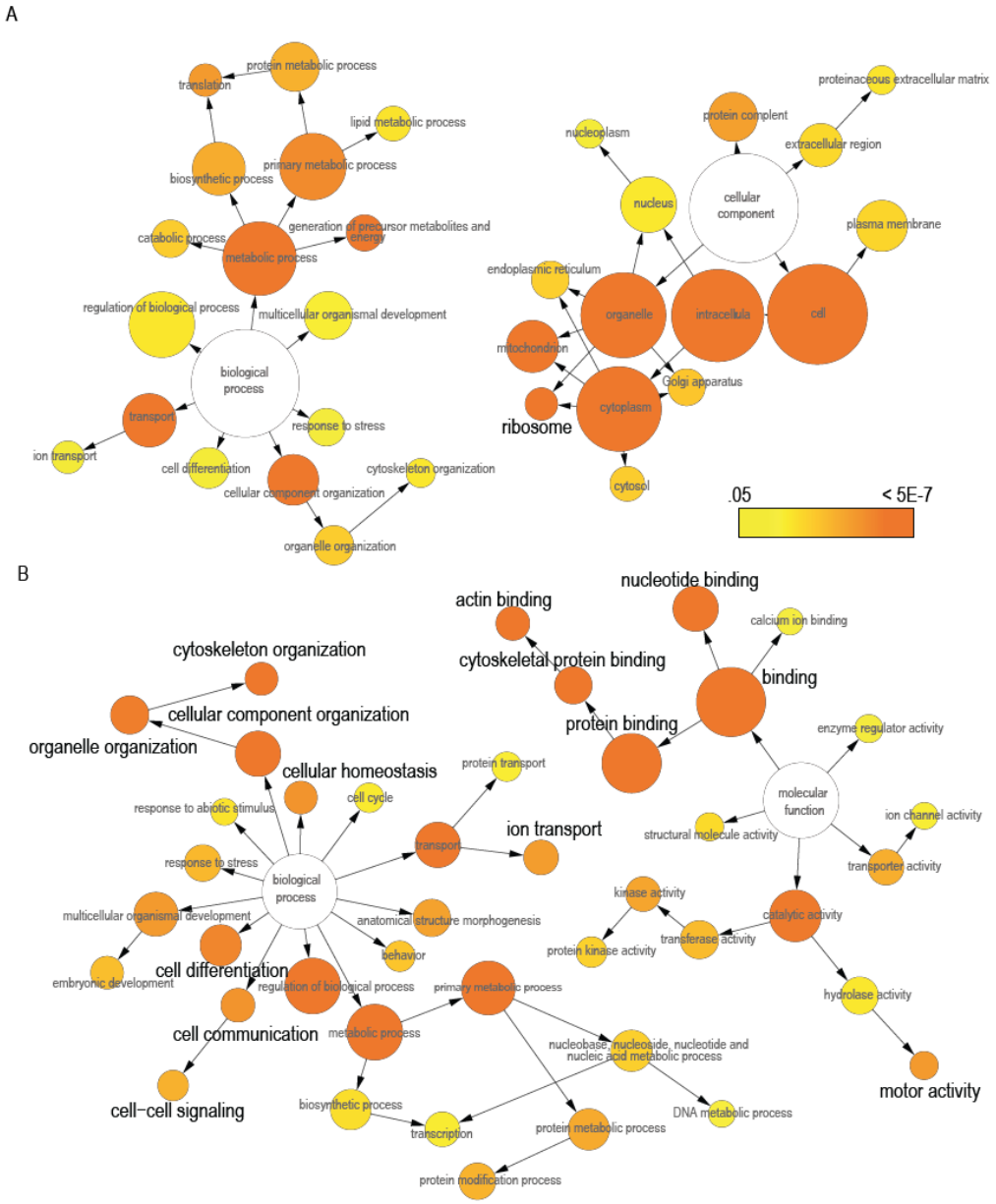

Figure 3: Translationally regulated genes show enrichment in specific Gene Ontology categories.

a) Exploratory GO pathway analysis of downregulated genes identifies trends for transcripts in key metabolic processes (e.g. mitochondrial and ribosomal transcripts) showing changes in ribosome occupancy.

b) Exploratory GO pathway analysis of upregulated genes indicates transcripts related to cytoskeleton/ actin binding, motor function, ion transport, and cell-cell signaling as showing robust increases in ribosome occupancy.

Grey fonts: p<.05 for categorical enrichment compared to whole genome. Black fonts: p<.05 for categorical enrichment compared to only astrocyte enriched genes. Color scale indicates significance for hypergeometric test. Category size is scaled to the number of genes. Arrows represent parent-child relationships in GO terms.

bioRxiv preprint doi: https://doi.org/10.1101/2020.04.08.033027; this version posted April 9, 2020. The copyright holder for this preprint (which was not certified by peer review) is the author/funder, who has granted bioRxiv a license to display the preprint in perpetuity. It is made available under aCC-BY-NC-ND 4.0 International license.

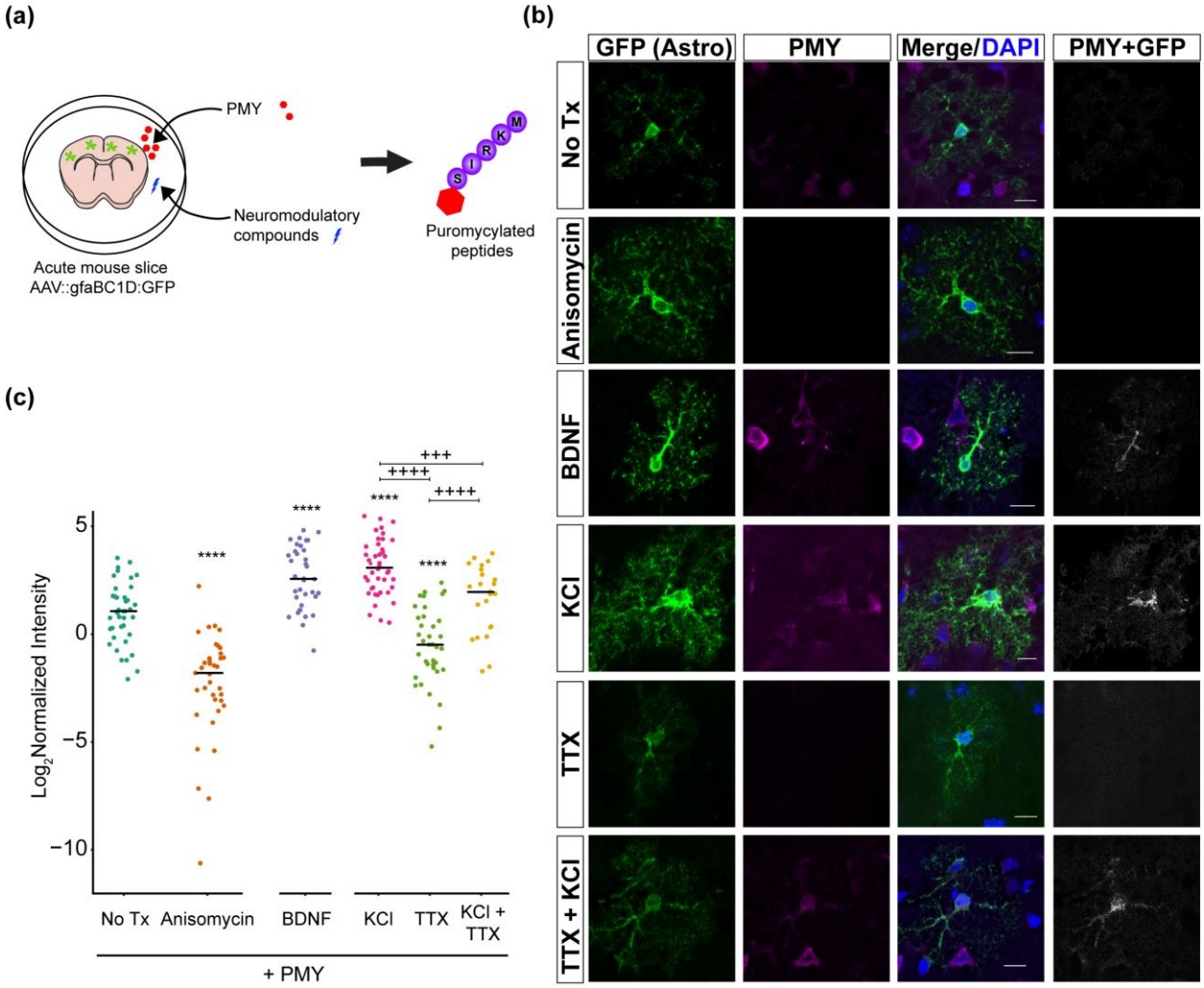

Figure 4: Astrocyte translation is modulated by BDNF and KCl

a) A schematic diagram showing an *ex vivo* translation assay. Acute brain slices can be treated with test compounds, and the resulting translational changes can be quantified using puromycin (PMY), which tags nascent peptides and serves as an epitope in the subsequent immunofluorescence staining experiment.

b) Representative confocal images of P21 cortical astrocytes after puromycylation. Astrocytes were labeled with AAV9:GFP (green, see methods) and incubated for 10 minutes with PMY and indicated pharmacological manipulations. IF for GFP (green) and PMY (magenta) was performed. Puro+GFP channel indicates colocalized pixels of PMY and GFP, and was enhanced for publication. Scale bars = 10µm.

c) Quantification of PMY intensity in GFP astrocytes. Normalized intensity was calculated by dividing PMY intensity by GFP area (pixels). Anova was performed to determine effect of condition, $F(5,211)=53.389$, $p<2.2E-16$. Post-hoc pairwise t-tests were performed. Asterisks indicate comparison to No Tx (PMY only), plus signs indicate comparisons within KCl and TTX conditions. $^{+++}p<0.005$, $^{****/++++}p<0.001$. N_{cells}(condition) = 40(No Tx), 37(Anisomycin), 36(BDNF), 44(KCl), 37(TTX), 23(KCl + TTX).

bioRxiv preprint doi: https://doi.org/10.1101/2020.04.08.033027; this version posted April 9, 2020. The copyright holder for this preprint (which was not certified by peer review) is the author/funder, who has granted bioRxiv a license to display the preprint in perpetuity. It is made available under aCC-BY-NC-ND 4.0 International license.

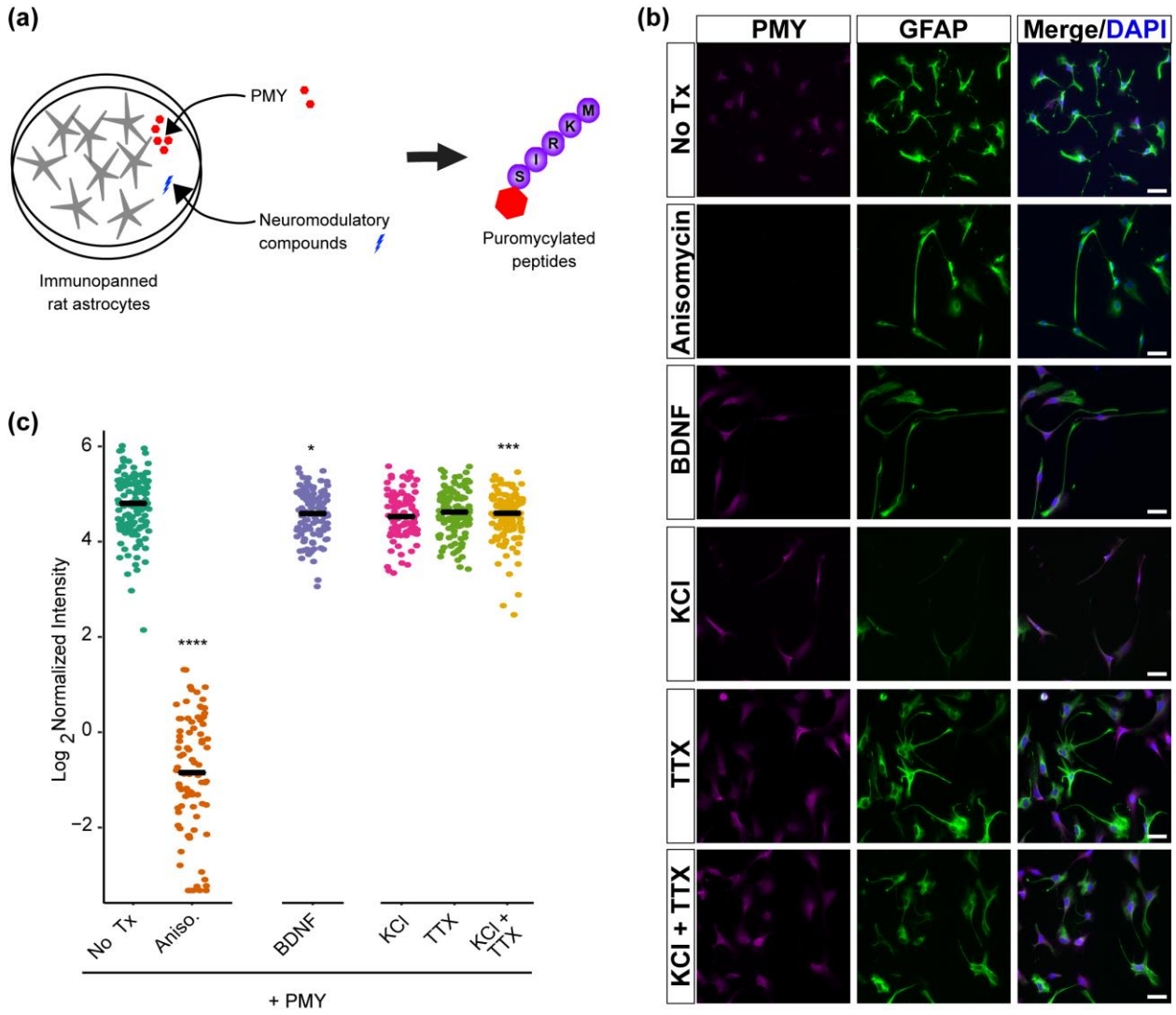

Figure 5: Impact of BDNF and KCl on astrocyte translation requires neurons

a) A schematic diagram of an assay for astrocyte-specific translation. Purified astrocytes are treated with test compounds, and the resulting translational response is measured using puromycin (PMY), which tags nascent peptides and is visualized in the subsequent immunofluorescence staining experiment.

b) Representative fields of immunopanned astrocytes, stained for puromycin and GFAP. Scale bar = 50µm.

c) Quantification of PMY intensity in astrocytes. Mean intensity (signal/area) was calculated for individual cells. Pairwise t-tests were performed compared to No Tx. ****$p<0.001$, ***$p<0.005$, *$p<0.05$. N_{cells}(condition) = 129 (No Tx, i.e. PMY only), 87 (Anisomycin), 97 (KCl), 120 (TTX), 104 (BDNF), 111 (KCl+TTX).

bioRxiv preprint doi: https://doi.org/10.1101/2020.04.08.033027; this version posted April 9, 2020. The copyright holder for this preprint (which was not certified by peer review) is the author/funder, who has granted bioRxiv a license to display the preprint in perpetuity. It is made available under aCC-BY-NC-ND 4.0 International license.

Supplemental Material

Supplemental Table 1: TRAP enriched transcripts

A list of 3409 transcripts enriched by TRAP in any one of three comparisons: ($TRAPseq^{All}$ vs $RNAseq^{All}$), or ($TRAPseq^{PTZ}$ vs $RNAseq^{PTZ}$), or ($TRAPseq^{Sal}$ vs $RNAseq^{Sal}$). Table includes columns for Ensembl gene IDs, Ensembl gene name, full gene name, Log2 Fold Change (Log2FC), EdgeR p-value and FDR corrected p-value for each of these comparisons.

Supplemental Table 2: Transcripts that respond to PTZ transcriptionally

A list of 23 genes altered transcriptionally by PTZ ($RNAseq^{PTZ}$ vs $RNAseq^{Sal}$). Table includes columns for Ensembl gene IDs, Ensembl gene name, full gene name, Log2 Fold Change (Log2FC), EdgeR p-value and FDR corrected p-value for this comparison.

Supplemental Table 3: Transcripts that respond to PTZ translationally

A list of transcripts with upregulated (n=102) or downregulated (n=315) ribosomal occupancy in response to PTZ ($TRAPseq^{PTZ}$ vs $TRAPseq^{Sal}$), filtered to remove those responding transcriptionally (Supplemental Table 2), and to only include those enriched in TRAP (Supplemental Table 3). Table includes columns for Ensembl gene IDs, Ensembl gene name, full gene name, Log2 Fold Change (Log2FC), EdgeR p-value and FDR corrected p-value for this comparison.

Supplemental Table 4: Mean expression and results of all comparisons across all expressed genes

A list of 11,593 genes that were measurably expressed in the experiment (CPM>5 in at least 3 out of 12 samples), with columns for Ensembl gene IDs, Ensembl gene name, full gene name, the p-value, FDR, and Log2FC results of any EdgeR comparisons described above, and mean expression for each sample type in CPM. Also included are columns (TRUE/FALSE) for whether the gene was considered TRAP enriched (i.e. on Supplemental Table 1) or transcriptionally responsive (Supplemental Table 2).

Supplemental Table 5: Full results tables for BiNGO pathway analysis.

Four sheets with full Cytoscape/BiNGO outputs using GOSlims pathways. Upregulated and downregulated genes from Supplemental Table 3 were tested using a reference set of either the whole mouse genome, or filtering the reference to include only the astrocyte TRAP enriched genes (Supplemental Table 1 – “astro back” sheets).

Supplemental Table 6: Selected results from COMPBIO analysis

Genes found within each theme, along with overall theme score, and the score for each individual gene within a theme as produced by COMPBIO analysis.

bioRxiv preprint doi: https://doi.org/10.1101/2020.04.08.033027; this version posted April 9, 2020. The copyright holder for this preprint (which was not certified by peer review) is the author/funder, who has granted bioRxiv a license to display the preprint in perpetuity. It is made available under aCC-BY-NC-ND 4.0 International license.

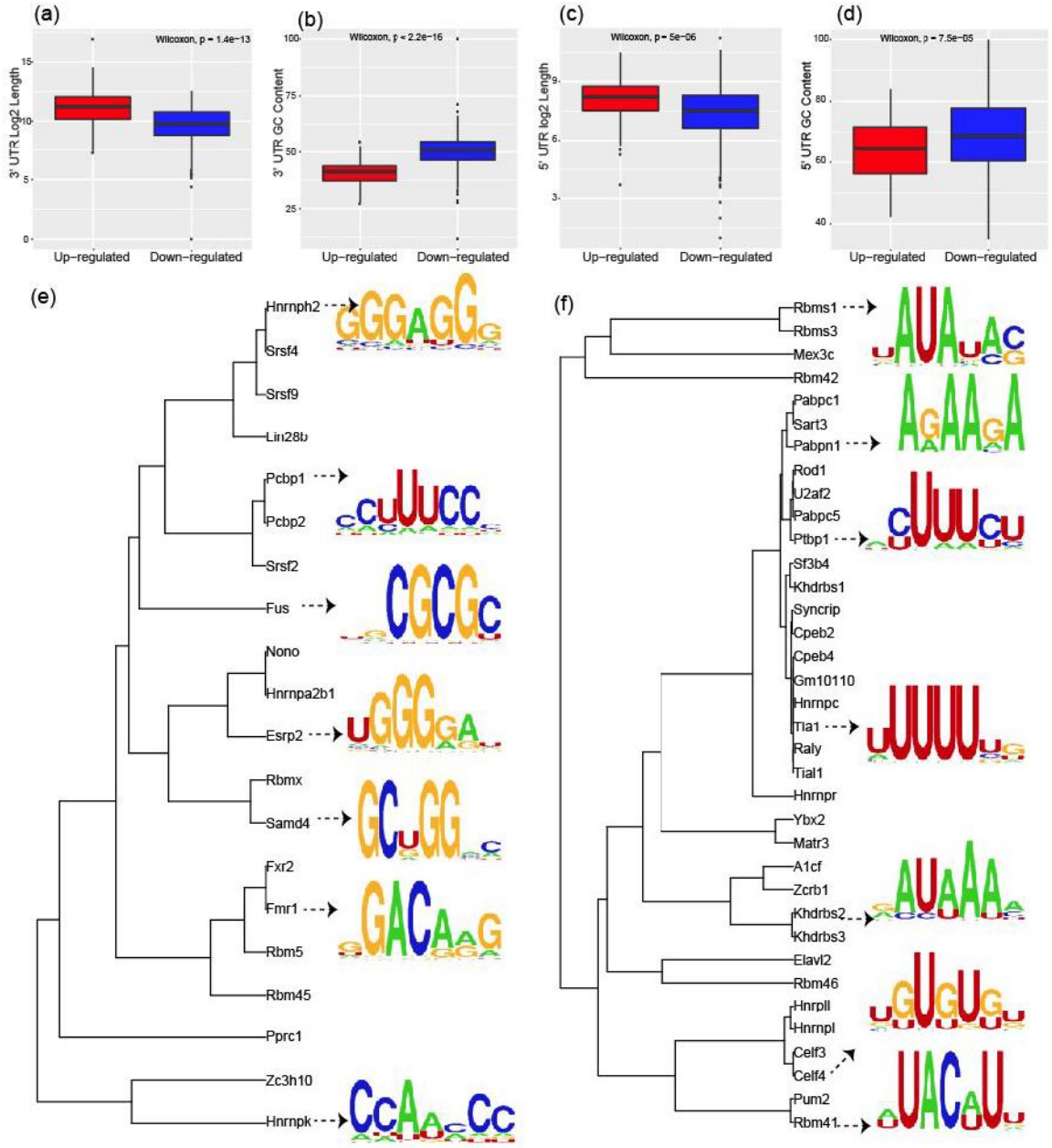

Supplemental Figure S1: Translationally regulated transcripts show distinct sequence features and recurrent motifs.

a-d) Translationally upregulated transcripts have significantly longer 3'UTR and 5'UTR (a and c) and lower GC contents in their 3'UTR and 5'UTR (b and d). e) AME analysis identifies dozens of RBPs with motifs that are significantly more common in 3'UTRs of the down-regulated transcript list. As many motifs are highly similar across RBPs, these have been clustered based on Euclidian distance in families of related factors. Examples of individual motifs for prototypical family members shown. *Motifs from RNAcompete data* (Ray et al., 2013) *http://hugheslab.ccbr.utoronto.ca/supplementary-data/RNAcompete_eukarya/Experiment_reports/RNAcompete_report_index.html* f) AME analysis identifies dozens of RBPs with motifs that are significantly more common in 3'UTRs of the up-regulated transcript list.

bioRxiv preprint doi: https://doi.org/10.1101/2020.04.08.033027; this version posted April 9, 2020. The copyright holder for this preprint (which was not certified by peer review) is the author/funder, who has granted bioRxiv a license to display the preprint in perpetuity. It is made available under aCC-BY-NC-ND 4.0 International license.

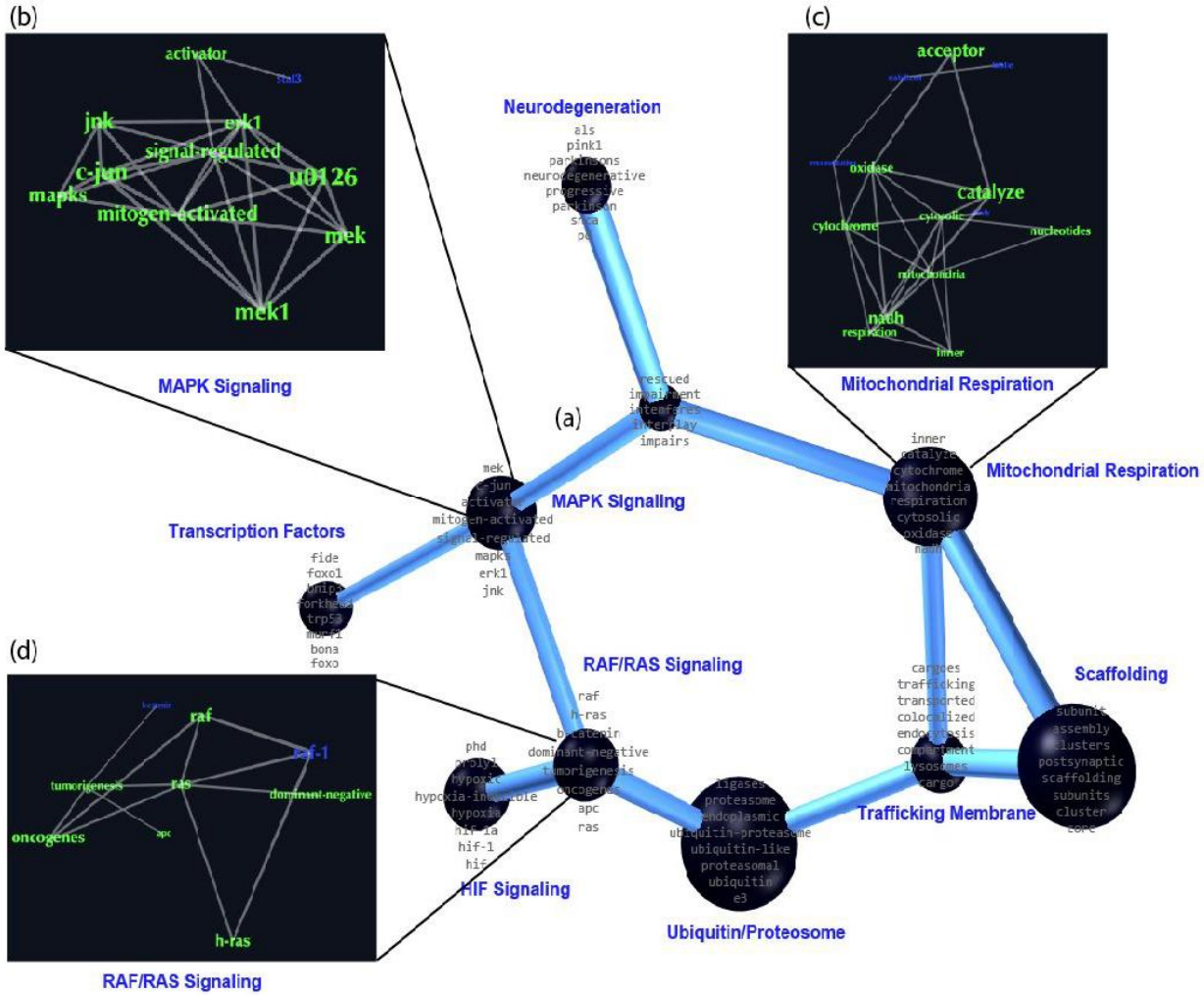

Supplemental Figure S2: Literature mining through language processing highlights potential regulatory pathways for translationally regulated transcripts.

a) Selected output of literature mining tool COMPBIO highlighting themes defined by terms co-occurring with the translationally regulated genes and with each other. Co-occurring terms are grouped into themes (nodes) that are connected by shared genes (edges). b-d) Relationships linking co-occurring terms within three example themes are shown. Supplemental table 6 includes the lists of genes connected with each theme, along with the scores as determined by permutation testing of similar sized lists of genes.

bioRxiv preprint doi: https://doi.org/10.1101/2020.04.08.033027; this version posted April 9, 2020. The copyright holder for this preprint (which was not certified by peer review) is the author/funder, who has granted bioRxiv a license to display the preprint in perpetuity. It is made available under aCC-BY-NC-ND 4.0 International license.

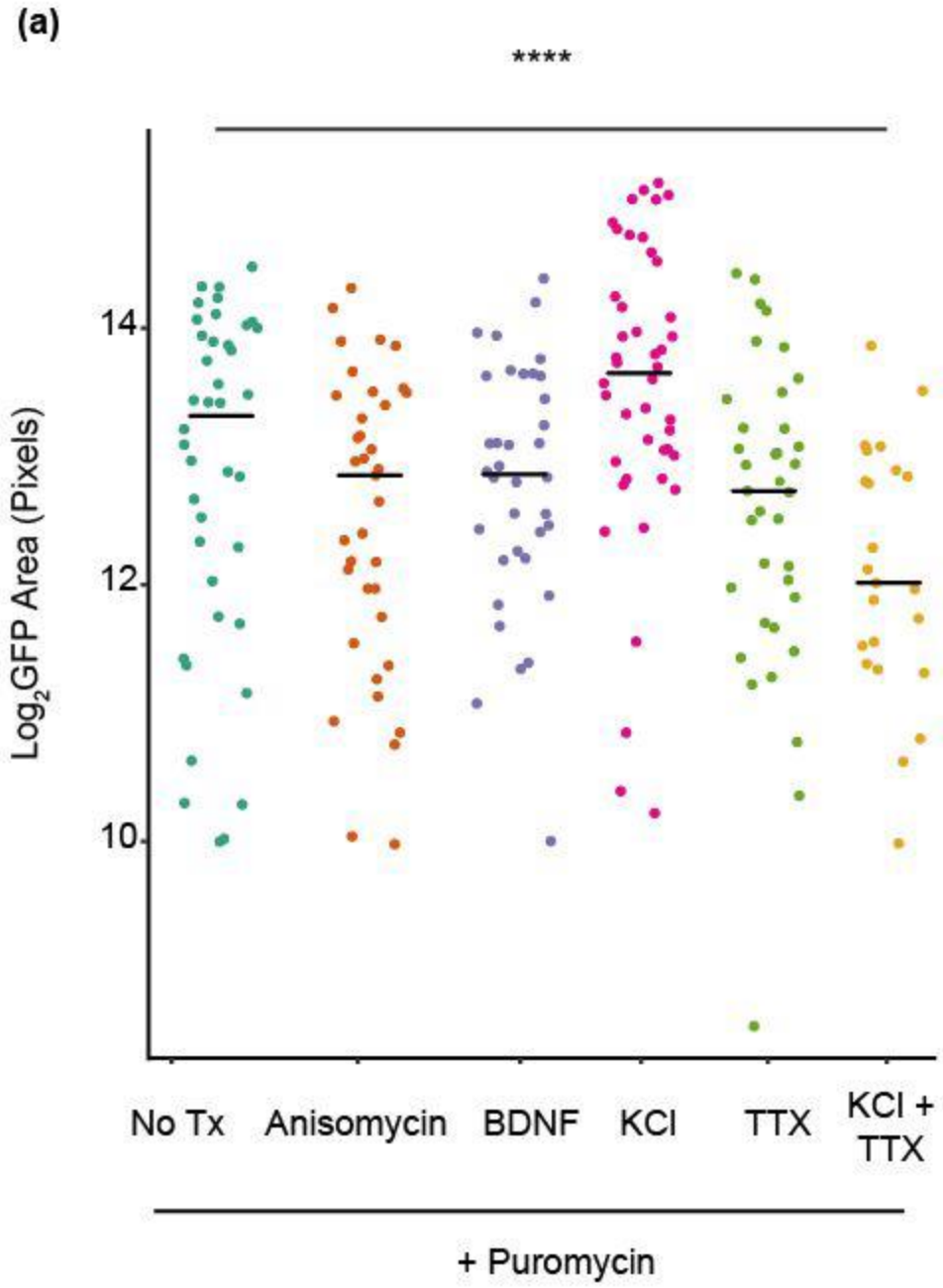

Supplemental Figure S3: KCl depolarization alters size of astrocytes.

a) Quantification of GFP pixel area of cells from Figure 4a. ANOVA was performed to determine the effect of conditions, F(5,211)=5.7716, p=5.13E-5.

bioRxiv preprint doi: https://doi.org/10.1101/2020.04.08.033027; this version posted April 9, 2020. The copyright holder for this preprint (which was not certified by peer review) is the author/funder, who has granted bioRxiv a license to display the preprint in perpetuity. It is made available under aCC-BY-NC-ND 4.0 International license.

References

Abrahams, B.S., Arking, D.E., Campbell, D.B., Mefford, H.C., Morrow, E.M., Weiss, L.A., Menashe, I., Wadkins, T., Banerjee-Basu, S., and Packer, A. (2013). SFARI Gene 2.0: a community-driven knowledgebase for the autism spectrum disorders (ASDs). Mol. Autism *4*, 36.

Agranoff, B.W., Davis, R.E., and Brink, J.J. (1966). Chemical studies on memory fixation in goldfish. Brain Res. *1*, 303–309.

Aroeira, R.I., Sebastião, A.M., and Valente, C.A. (2015). BDNF, via truncated TrkB receptor, modulates GlyT1 and GlyT2 in astrocytes. Glia *63*, 2181–2197.

Balkowiec, A., and Katz, D.M. (2000). Activity-dependent release of endogenous brain-derived neurotrophic factor from primary sensory neurons detected by ELISA in situ. J. Neurosci. Off. J. Soc. Neurosci. *20*, 7417–7423.

Bolger, A.M., Lohse, M., and Usadel, B. (2014). Trimmomatic: a flexible trimmer for Illumina sequence data. Bioinformatics *30*, 2114–2120.

Boulay, A.-C., Saubaméa, B., Adam, N., Chasseigneaux, S., Mazaré, N., Gilbert, A., Bahin, M., Bastianelli, L., Blugeon, C., Perrin, S., et al. (2017). Translation in astrocyte distal processes sets molecular heterogeneity at the gliovascular interface. Cell Discov. *3*, 17005.

Cajigas, I.J., Tushev, G., Will, T.J., Dieck, S. tom, Fuerst, N., and Schuman, E.M. (2012). The Local Transcriptome in the Synaptic Neuropil Revealed by Deep Sequencing and High-Resolution Imaging. Neuron *74*, 453–466.

Chai, H., Diaz-Castro, B., Shigetomi, E., Monte, E., Octeau, J.C., Yu, X., Cohn, W., Rajendran, P.S., Vondriska, T.M., Whitelegge, J.P., et al. (2017). Neural Circuit-Specialized Astrocytes: Transcriptomic, Proteomic, Morphological, and Functional Evidence. Neuron *95*, 531-549.e9.

Charles, A.C., Merrill, J.E., Dirksen, E.R., and Sandersont, M.J. (1991). Intercellular signaling in glial cells: Calcium waves and oscillations in response to mechanical stimulation and glutamate. Neuron *6*, 983–992.

Chen, P.B., Kawaguchi, R., Blum, C., Achiro, J.M., Coppola, G., O'Dell, T.J., and Martin, K.C. (2017). Mapping Gene Expression in Excitatory Neurons during Hippocampal Late-Phase Long-Term Potentiation. Front. Mol. Neurosci. *10*, 39.

Cho, J., Yu, N.-K., Choi, J.-H., Sim, S.-E., Kang, S.J., Kwak, C., Lee, S.-W., Kim, J., Choi, D.I., Kim, V.N., et al. (2015). Multiple repressive mechanisms in the hippocampus during memory formation. Science *350*, 82–87.

Colombo, E., Cordiglieri, C., Melli, G., Newcombe, J., Krumbholz, M., Parada, L.F., Medico, E., Hohlfeld, R., Meinl, E., and Farina, C. (2012). Stimulation of the neurotrophin receptor TrkB on astrocytes drives nitric oxide production and neurodegeneration. J. Exp. Med. *209*, 521–535.

bioRxiv preprint doi: https://doi.org/10.1101/2020.04.08.033027; this version posted April 9, 2020. The copyright holder for this preprint (which was not certified by peer review) is the author/funder, who has granted bioRxiv a license to display the preprint in perpetuity. It is made available under aCC-BY-NC-ND 4.0 International license.

Dalal, J.S., Yang, C., Sapkota, D., Lake, A.M., O'Brien, D.R., and Dougherty, J.D. (2017). Quantitative Nucleotide Level Analysis of Regulation of Translation in Response to Depolarization of Cultured Neural Cells. Front. Mol. Neurosci. *10*, 9.

Dieni, S., Matsumoto, T., Dekkers, M., Rauskolb, S., Ionescu, M.S., Deogracias, R., Gundelfinger, E.D., Kojima, M., Nestel, S., Frotscher, M., et al. (2012). BDNF and its pro-peptide are stored in presynaptic dense core vesicles in brain neurons. J. Cell Biol. *196*, 775–788.

Dieterich, D.C., Hodas, J.J.L., Gouzer, G., Shadrin, I.Y., Ngo, J.T., Triller, A., Tirrell, D.A., and Schuman, E.M. (2010). In situ visualization and dynamics of newly synthesized proteins in rat hippocampal neurons. Nat. Neurosci. *13*, 897–905.

Dobin, A., Davis, C.A., Schlesinger, F., Drenkow, J., Zaleski, C., Jha, S., Batut, P., Chaisson, M., and Gingeras, T.R. (2013). STAR: ultrafast universal RNA-seq aligner. Bioinforma. Oxf. Engl. *29*, 15–21.

Dougherty, J.D., Fomchenko, E.I., Akuffo, A.A., Schmidt, E., Helmy, K.Y., Bazzoli, E., Brennan, C.W., Holland, E.C., and Milosevic, A. (2012). Candidate pathways for promoting differentiation or quiescence of oligodendrocyte progenitor-like cells in glioma. Cancer Res. *72*, 4856–4868.

Doyle, J.P., Dougherty, J.D., Heiman, M., Schmidt, E.F., Stevens, T.R., Ma, G., Bupp, S., Shrestha, P., Shah, R.D., Doughty, M.L., et al. (2008). Application of a translational profiling approach for the comparative analysis of CNS cell types. Cell *135*, 749–762.

Farris, S., Lewandowski, G., Cox, C.D., and Steward, O. (2014). Selective Localization of Arc mRNA in Dendrites Involves Activity- and Translation-Dependent mRNA Degradation. J. Neurosci. *34*, 4481–4493.

Flexner, J.B., Flexner, L.B., and Stellar, E. (1963). Memory in Mice as Affected by Intracerebral Puromycin. Science *141*, 57–59.

Foo, L.C., Allen, N.J., Bushong, E.A., Ventura, P.B., Chung, W.-S., Zhou, L., Cahoy, J.D., Daneman, R., Zong, H., Ellisman, M.H., et al. (2011). Development of a method for the purification and culture of rodent astrocytes. Neuron *71*, 799–811.

Hafner, A.-S., Donlin-Asp, P.G., Leitch, B., Herzog, E., and Schuman, E.M. (2019). Local protein synthesis is a ubiquitous feature of neuronal pre- and postsynaptic compartments. Science *364*, eaau3644.

Hardingham, G.E., Arnold, F.J.L., and Bading, H. (2001). Nuclear calcium signaling controls CREB-mediated gene expression triggered by synaptic activity. Nat. Neurosci. *4*, 261.

Hasel, P., Dando, O., Jiwaji, Z., Baxter, P., Todd, A.C., Heron, S., Márkus, N.M., McQueen, J., Hampton, D.W., Torvell, M., et al. (2017). Neurons and neuronal activity control gene expression in astrocytes to regulate their development and metabolism. Nat. Commun. *8*, 15132.

Heiman, M., Schaefer, A., Gong, S., Peterson, J.D., Day, M., Ramsey, K.E., Suárez-Fariñas, M., Schwarz, C., Stephan, D.A., Surmeier, D.J., et al. (2008). A translational profiling approach for the molecular characterization of CNS cell types. Cell *135*, 738–748.

bioRxiv preprint doi: https://doi.org/10.1101/2020.04.08.033027; this version posted April 9, 2020. The copyright holder for this preprint (which was not certified by peer review) is the author/funder, who has granted bioRxiv a license to display the preprint in perpetuity. It is made available under aCC-BY-NC-ND 4.0 International license.

Hrvatin, S., Hochbaum, D.R., Nagy, M.A., Cicconet, M., Robertson, K., Cheadle, L., Zilionis, R., Ratner, A., Borges-Monroy, R., Klein, A.M., et al. (2018). Single-cell analysis of experience-dependent transcriptomic states in the mouse visual cortex. Nat. Neurosci. *21*, 120–129.

Kalish, B.T., Cheadle, L., Hrvatin, S., Nagy, M.A., Rivera, S., Crow, M., Gillis, J., Kirchner, R., and Greenberg, M.E. (2018). Single-cell transcriptomics of the developing lateral geniculate nucleus reveals insights into circuit assembly and refinement. Proc. Natl. Acad. Sci. 201717871.

Kang, H., and Schuman, E.M. (1996). A requirement for local protein synthesis in neurotrophin-induced hippocampal synaptic plasticity. Science *273*, 1402–1406.

Langmead, B., and Salzberg, S.L. (2012). Fast gapped-read alignment with Bowtie 2. Nat. Methods *9*, 357–359.

Leal, G., Comprido, D., and Duarte, C.B. (2014). BDNF-induced local protein synthesis and synaptic plasticity. Neuropharmacology *76, Part C*, 639–656.

Li, J., Khankan, R.R., Caneda, C., Godoy, M.I., Haney, M.S., Krawczyk, M.C., Bassik, M.C., Sloan, S.A., and Zhang, Y. (2019). Astrocyte-to-astrocyte contact and a positive feedback loop of growth factor signaling regulate astrocyte maturation. Glia *67*, 1571–1597.

Maere, S., Heymans, K., and Kuiper, M. (2005). BiNGO: a Cytoscape plugin to assess overrepresentation of gene ontology categories in biological networks. Bioinforma. Oxf. Engl. *21*, 3448–3449.

McLeay, R.C., and Bailey, T.L. (2010). Motif Enrichment Analysis: a unified framework and an evaluation on ChIP data. BMC Bioinformatics *11*, 165.

Molotkov, D., Zobova, S., Arcas, J.M., and Khiroug, L. (2013). Calcium-induced outgrowth of astrocytic peripheral processes requires actin binding by Profilin-1. Cell Calcium *53*, 338–348.

Müller, A., Stellmacher, A., Freitag, C.E., Landgraf, P., and Dieterich, D.C. (2015). Monitoring Astrocytic Proteome Dynamics by Cell Type-Specific Protein Labeling. PloS One *10*, e0145451.

Ouwenga, R., Lake, A.M., O'Brien, D., Mogha, A., Dani, A., and Dougherty, J.D. (2017). Transcriptomic Analysis of Ribosome-Bound mRNA in Cortical Neurites In Vivo. J. Neurosci. *37*, 8688–8705.

Ouwenga, R., Lake, A.M., Aryal, S., Lagunas, T., and Dougherty, J.D. (2018). The Differences in Local Translatome across Distinct Neuron Types Is Mediated by Both Baseline Cellular Differences and Post-transcriptional Mechanisms. ENeuro *5*, ENEURO.0320-18.2018.

Pardo, L., Valor, L.M., Eraso-Pichot, A., Barco, A., Golbano, A., Hardingham, G.E., Masgrau, R., and Galea, E. (2017). CREB Regulates Distinct Adaptive Transcriptional Programs in Astrocytes and Neurons. Sci. Rep. *7*, 6390.

Perea, G., Navarrete, M., and Araque, A. (2009). Tripartite synapses: astrocytes process and control synaptic information. Trends Neurosci. *32*, 421–431.

bioRxiv preprint doi: https://doi.org/10.1101/2020.04.08.033027; this version posted April 9, 2020. The copyright holder for this preprint (which was not certified by peer review) is the author/funder, who has granted bioRxiv a license to display the preprint in perpetuity. It is made available under aCC-BY-NC-ND 4.0 International license.

Perego, C., Vanoni, C., Bossi, M., Massari, S., Basudev, H., Longhi, R., and Pietrini, G. (2000). The GLT-1 and GLAST glutamate transporters are expressed on morphologically distinct astrocytes and regulated by neuronal activity in primary hippocampal cocultures. J. Neurochem. *75*, 1076–1084.

Pilaz, L.-J., Lennox, A.L., Rouanet, J.P., and Silver, D.L. (2016). Dynamic mRNA Transport and Local Translation in Radial Glial Progenitors of the Developing Brain. Curr. Biol. CB *26*, 3383–3392.

Ray, D., Kazan, H., Cook, K.B., Weirauch, M.T., Najafabadi, H.S., Li, X., Gueroussov, S., Albu, M., Zheng, H., Yang, A., et al. (2013). A compendium of RNA-binding motifs for decoding gene regulation. Nature *499*, 172–177.

Reddy, A.S., O'Brien, D., Pisat, N., Weichselbaum, C.T., Sakers, K., Lisci, M., Dalal, J.S., and Dougherty, J.D. (2017). A Comprehensive Analysis of Cell Type–Specific Nuclear RNA From Neurons and Glia of the Brain. Biol. Psychiatry *81*, 252–264.

Rieger, M.A., King, D.M., Cohen, B.A., and Dougherty, J.D. (2018). CLIP-Seq and massively parallel functional analysis of the CELF6 RNA binding protein reveals a role in destabilizing synaptic gene mRNAs through interaction with 3'UTR elements in vivo. BioRxiv 401604.

Robinson, M.D., McCarthy, D.J., and Smyth, G.K. (2010). edgeR: a Bioconductor package for differential expression analysis of digital gene expression data. Bioinforma. Oxf. Engl. *26*, 139–140.

Sakers, K., Lake, A.M., Khazanchi, R., Ouwenga, R., Vasek, M.J., Dani, A., and Dougherty, J.D. (2017). Astrocytes locally translate transcripts in their peripheral processes. Proc. Natl. Acad. Sci. U. S. A. *114*, E3830–E3838.

Sanz, E., Yang, L., Su, T., Morris, D.R., McKnight, G.S., and Amieux, P.S. (2009). Cell-type-specific isolation of ribosome-associated mRNA from complex tissues. Proc. Natl. Acad. Sci. U. S. A. *106*, 13939–13944.

Satterstrom, F.K., Kosmicki, J.A., Wang, J., Breen, M.S., Rubeis, S.D., An, J.-Y., Peng, M., Collins, R.L., Grove, J., Klei, L., et al. (2018). Novel genes for autism implicate both excitatory and inhibitory cell lineages in risk. BioRxiv 484113.

Schipke, C.G., and Kettenmann, H. (2004). Astrocyte responses to neuronal activity. Glia *47*, 226–232.

Song, Y., and Gunnarson, E. (2012). Potassium Dependent Regulation of Astrocyte Water Permeability Is Mediated by cAMP Signaling. PLOS ONE *7*, e34936.

Steward, O., Farris, S., Pirbhoy, P.S., Darnell, J., and Driesche, S.J.V. (2015). Localization and local translation of Arc/Arg3.1 mRNA at synapses: some observations and paradoxes. Front. Mol. Neurosci. *7*.

Swanson, R.A., Liu, J., Miller, J.W., Rothstein, J.D., Farrell, K., Stein, B.A., and Longuemare, M.C. (1997). Neuronal regulation of glutamate transporter subtype expression in astrocytes. J. Neurosci. Off. J. Soc. Neurosci. *17*, 932–940.

Wang, X., Lou, N., Xu, Q., Tian, G.-F., Peng, W.G., Han, X., Kang, J., Takano, T., and Nedergaard, M. (2006). Astrocytic Ca2+ signaling evoked by sensory stimulation in vivo. Nat. Neurosci. *9*, 816–823.

bioRxiv preprint doi: https://doi.org/10.1101/2020.04.08.033027; this version posted April 9, 2020. The copyright holder for this preprint (which was not certified by peer review) is the author/funder, who has granted bioRxiv a license to display the preprint in perpetuity. It is made available under aCC-BY-NC-ND 4.0 International license.

Wang, Y., Hagel, C., Hamel, W., Müller, S., Kluwe, L., and Westphal, M. (1998). Trk A, B, and C are commonly expressed in human astrocytes and astrocytic gliomas but not by human oligodendrocytes and oligodendroglioma. Acta Neuropathol. (Berl.) *96*, 357–364.

Yap, E.-L., and Greenberg, M.E. (2018). Activity-Regulated Transcription: Bridging the Gap between Neural Activity and Behavior. Neuron *100*, 330–348.

Zafra, F., Hengerer, B., Leibrock, J., Thoenen, H., and Lindholm, D. (1990). Activity dependent regulation of BDNF and NGF mRNAs in the rat hippocampus is mediated by non-NMDA glutamate receptors. EMBO J. *9*, 3545–3550.

Zhang, Y., Chen, K., Sloan, S.A., Bennett, M.L., Scholze, A.R., O'Keeffe, S., Phatnani, H.P., Guarnieri, P., Caneda, C., Ruderisch, N., et al. (2014). An RNA-sequencing transcriptome and splicing database of glia, neurons, and vascular cells of the cerebral cortex. J. Neurosci. Off. J. Soc. Neurosci. *34*, 11929–11947.

Zhang, Y., Sloan, S.A., Clarke, L.E., Caneda, C., Plaza, C.A., Blumenthal, P.D., Vogel, H., Steinberg, G.K., Edwards, M.S.B., Li, G., et al. (2016). Purification and Characterization of Progenitor and Mature Human Astrocytes Reveals Transcriptional and Functional Differences with Mouse. Neuron *89*, 37–53.